Effects of protein concentration on IgE receptor mobility in rat basophilic leukemia cell plasma membranes

James L. Thomas, Toni J. Feder, and Watt W. Webb

Department of Physics and School of Applied and Engineering Physics, Cornell University, Ithaca, New York 14853 USA

ABSTRACT The ability of variations of membrane protein concentrations to modulate the lateral diffusion rate of an exemplary membrane protein has been studied in healthy and osmotically shocked cultured cells of the rat basophilic leukemia cell line, 2H3 subclone. Cell surface protein was redistributed by the method of in situ electrophoresis; exposure to electric fields of 1.25–5 V/cm results in cathodal migration of the majority of the surface proteins on this cell type (Ryan, T. A., J. Myers, D. Holowka, B. Baird, and W. W. Webb. Science [Wash. DC]. 239:61–64). Even in these small fields, the steady-state distribution becomes "crowded" with more than an 80% protein occupancy of accessible membrane area at the cathodal end of these spheroidal cells, and the anodal end becomes significantly depleted. We have employed fringe pattern fluorescence photobleaching with CCD imaging detection to measure lateral diffusion coefficients of the liganded IgE receptor on both crowded and uncrowded regions of individual rat basophilic leukemia cells. We find no significant difference in lateral diffusion rates in these regions. Cells swollen by hypoosmotic stress exhibit faster diffusion overall, with the uncrowded regions having a significantly greater increase in diffusion coefficient than the crowded regions. These results are consistent with the partial or total release of cytoskeletal constraints to membrane protein diffusion induced by osmotic stress.

INTRODUCTION

Measured values of the lateral tracer diffusion coefficients, D, of proteins in cell plasma membranes are two to three orders of magnitude slower than predicted by hydrodynamic theory for lipid membranes (Saffman and Delbrück, 1975). Many researchers have worked to identify the causes of slowed protein diffusion. Among the factors that may contribute are interactions of membrane proteins with cytoskeletal elements, interactions with the extracellular matrix or glycocalyx, and interactions among membrane proteins (Webb et al., 1981). Here we present experiments investigating the role of membrane protein concentration in modulating protein diffusion on living cells in culture, including osmotically swollen (bulbous) cells.

All of the factors mentioned above have been shown to be capable of affecting lateral diffusion. For example, Zhang et al. (1990) have constructed chimeric membrane proteins and were able to slow diffusion by replacing either the transmembrane or the extracellular portion of a rapidly diffusing protein ($D \sim 10^{-9}$ cm²/s) with the corresponding region of a slowly diffusing protein ($D \sim 10^{-10}$ cm²/s). In their work, the slowing of diffusion may have been due to specific, "lock-and-key" interactions felt by the slow diffuser but not by the fast diffuser. However, a number of measurements in reconstituted bilayer systems, and computer experiments, suggest that even in the absence of specific protein–protein interactions, protein diffusion is slowed in crowded membranes. Tank et al. (1982a) found a threefold reduction in the lateral diffusion coefficient of gramicidin C in dimyristoyl phosphatidylcholine bilayers, at high concentration of protein. Peters and Cherry (1982) report that the diffusion coefficient of reconstituted bacteriorhodopsin decreases by a factor of 2.5 as the protein concentration is increased to 1.1 mol%. Computer experiments using a "lattice gas" model of proteins in a cell membrane also show dramatic reductions in D at high protein concentrations (Pink, 1985; Saxton, 1987; Donaldson, 1989).

These reconstituted systems, and most computer experiments, do not incorporate cytoskeleton. Yet the cytoskeleton may dominate diffusive behavior in vivo. Experiments by Tank et al. (1982b) on plasma membrane blebs showed a 100-fold increase in the diffusion coefficient of Con A receptors over that observed on normal cell membrane. These blebs were conspicuously devoid of cytoskeleton, which led those researchers to suggest that cytoskeleton was responsible for slowed diffusion on the intact cell surface.

Motivated by concerns over the role of cytoskeleton in determining diffusion coefficients, we made measurements of the effect of protein crowding on hypoosmotically shocked cells as well as on normal cells. We utilize a tumor mast cell line, the rat basophilic leukemia

(RBL) cell. Under hypoosmotic shock, these spherical cells swell to nearly double their normal diameter, and the plasma membrane detaches from the actin cytoskeleton, as observed by fluorescence staining of F-actin.

To investigate the concentration dependence of diffusion in normal and bulbous RBL cells, we have combined the techniques of in situ electrophoresis, to redistribute cell surface proteins, and pattern photobleaching recovery, to measure protein tracer diffusion coefficients. Jaffe (1977) predicted that the application of a tangential electric field would laterally redistribute charged membrane constituents on cell surfaces. Field-induced accumulation of cell surface proteins was observed by Poo et al. (1979) with Con A receptors on *Xenopus* myotomal cells and later by McCloskey et al. (1984) with the IgE-Fc receptor of RBL cells. Ryan et al. (1988) then demonstrated that, on RBL cells, nonspecifically labeled cell surface proteins generally undergo a migration toward the cathode in an electric field, leading to an overall gradient in the concentration of protein in the cell membrane. (This result may be explained by the electroosmotic hypothesis of McLaughlin and Poo [1981].) We have utilized this technology to obtain RBL cells with local protein concentrations that are more than five times the original, preelectrophoresis concentrations. We then use pattern photobleaching to measure diffusion coefficients at both the crowded (cathodal) and dilute (anodal) poles of single cells. We find no apparent dependence of protein diffusion on protein concentration on normal cells. However, we do find that the lateral diffusion coefficients do decrease with increasing protein concentration on osmotically shocked cells.

MATERIALS

FITC conjugated to rat IgE (FITC-IgE$_R$), tetramethyl rhodamine isothiocyanate (TRITC), and IgE$_R$ were generous gifts of Drs. Barbara Baird and David Holowka. TRITC-IgE$_R$ was prepared by reacting IgE$_R$ (7 μM) in sodium phosphate buffer (61:39 0.2 M Na$_2$HPO$_4$/NaH$_2$PO$_4$, 1 mM EDTA, pH 8.0) with TRITC ($\sim$24 mM) for 24 h at room temperature (Menon et al., 1985). After the reaction, samples were dialyzed against several changes of buffer (same as above, with 0.1 M NaCl) for 48 h. The concentration of bound TRITC-IgE$_R$ was $\sim$4 μM, determined from the optical density at 556 nm.

A tritium release assay was performed to check whether the TRITC-IgE$_R$ preparation causes degranulation, a well-known response of RBL cells to cross-linking of the IgE$_R$ receptor complexes (IgE$_R$-R). Cells were preloaded with tritiated seratonin hydroxytriptamine and then incubated with TRITC-IgE$_R$. Even at 10 times the ratio of TRITC-IgE$_R$ to receptors used in our experiments, the release of tritium was negligible, suggesting that our TRITC-IgE$_R$ does not cause aggregation of IgE-R.

Rhodamine-labeled succinylated Con A (Rh-S-Con A) (E-Y Laboratories, Inc., San Mateo, CA) was used in postfield labeling experiments. Bodipy phallacidin (Molecular Probes, Inc., Eugene, OR) was used for labeling cytoskeletal actin filaments.

METHODS

Cell preparation

RBL cells (2H3 subclone) were generously provided by Drs. B. Baird and D. Holowka. They were grown adherent to flasks and 4–6 d after passage were harvested (mM: 135 NaCl, 5 KCl, 0.2 MgCl$_2$, 20 Hepes, and 1.5 EDTA), and then resuspended in Earle's MEM (Gibco Laboratories, Grand Island, NY) with 10% FCS and 2% 1 M Hepes buffer (MEM^{++}).

Fluorescent IgE$_R$ was bound to the high-affinity F$_c$ receptors on the cells by incubation with a 10-fold molar excess of TRITC-IgE$_R$ for $\sim$¾ h, rotating at 37°C. They were washed twice with MEM^{++} by gentle centrifugation and resuspension. IgE receptors comprise $\simeq$1% of the total surface protein on RBL cells; virtually all have bound IgE$_R$ after this process.

10 min plating in Tyrodes buffer (mM: 135 NaCl, 5 KCl, 1.8 CaCl$_2$, 1 MgCl$_2$, 5.6 glucose, 20 Hepes, and 5% gelatin) at 37°C permitted the cells to adhere to No. 1 coverslips while maintaining sphericity, as verified by the decreasing circumference seen when focusing either up or down. The cells were then rinsed and mounted in an electric field application chamber built for use on the Universal (Carl Zeiss, Inc., Thornwood, NY) microscope.

Postfield labeling

For postfield labeling, cells were not primed with IgE. After application of an electric field, coverslips were gently removed from the chamber by addition of buffer and then immediately placed on an aluminum block on ice and incubated with Rh-S-Con A at 100 μg/ml. This lectin binds to saccharides of glycosylated proteins of the cell surface. After 30 min the cells were fixed with acetone at 4°C. Coverslips were then mounted and the postfield label Con A distributions examined in the microscope.

Osmotic swelling of cells

Osmotic shock was induced by replacing the bathing medium (Tyrodes buffer) with distilled water after plating. After $\sim$10 min in water, the cell radius increases by a factor of 1.8 $\pm$ 0.3, with the projected surface area correspondingly increasing 3.2 times. Electron microscopy (Pfeiffer et al., 1985) has shown that the intact RBL cell has a microvillus membrane; it is the availability of the additional membrane present in the villi that allows the cells to expand so dramatically during osmotic shock.

The actin cytoskeleton was fluorescently labeled with Bodipy phallacidin using the technique of pinocytosis in hypoosmotic medium described by Okada and Rechsteiner (1982). Cells thus labeled were then placed in distilled water and examined in bright field as well as by fluorescence microscopy to verify that the cytoskeleton indeed becomes detached from the membrane upon being subjected to osmotic shock.

Electrophoresis

The electrophoresis chamber has a thin cell space of $\sim$150 μm (thickness of one No. 1 coverslip) above a heat-conducting sapphire plate and a pumped water cooling system. Water was at ambient temperature, $\sim$25°C. Bridges of agarose (UltraPure electrophoresis grade, Bethesda Research Laboratories, Gaithersburg, MD) made in Tyrodes buffer (or Tyrodes buffer diluted 10 times with distilled water, in the case of bulbous cells) separate the cell region from the platinum electrodes at the ends of the chamber to prevent contamination of the

cells by reactants from the electrodes (chamber dimensions: 0.6 cm deep × 5 cm long × 2.5 cm wide). Since the most electromobile electrode reaction product is H^+, we monitor the pH in the agarose with a trace amount of the indicator Phenol Red. As electrode products migrate toward the cell space, a color front moves through the agarose. Experiments are halted long before this pH change reaches the cells. Silver-chlorided silver wires probe the voltage drop across the cell space.

We applied fields of 1.25–20 V/cm to the cells. A thermocouple temperature probe was used to determine that the medium bathing the cells was never >3°C over ambient temperature. Photobleaching experiments were performed only after IgE_R-F_c complexes reached the equilibrium distribution in the applied field (≥ 10 min in field).

Bleaching optics

To measure tracer diffusion coefficients at each pole of a cell, an interference pattern photobleaching scheme was used (Davoust et al., 1982). The 514-nm line from an argon ion laser (Innova-6, Coherent, Inc., Palo Alto, CA) was split and recombined at low angle through the sample to produce an interference fringe pattern of 3-μm peak-to-peak spacing. Because of the increased size and the faster diffusion on osmotically swollen cells, the interference pattern spacing was increased to 6 μm. The exact pattern spacing was measured for each run. The optical path for the bleaching laser is illustrated in Fig. 1. The low angle at which the beams cross creates a fringe pattern >100 μm in extent along the optic axis, as was verified by direct measurement with fluorescent films.

After cells had reached a steady state in the applied electric field, a conventional epifluorescence image of a cell was taken with 546 nm illumination from a 100-W mercury arc lamp, Fig. 2 a. This image was used to determine the protein concentrations at the cathodal and anodal poles of the cell, as described in the following section. The cell was then briefly exposed to the bright interference fringes from the laser (<0.5 s, ~1 W of power in a field ~50 μm in diameter.) The fringe pattern irreversibly photobleaches the fluorescence in lines parallel to the applied electric field (Fig. 2 b). The mean cell surface fluorescence is reduced by about a factor of three, and the peak-to-trough modulation amplitude is typically 30–50% of the remaining fluorescence. Conventional epifluorescence images were taken after

photobleaching and were used to determine the diffusion coefficient of TRITC-IgE_R receptor complex. These postbleach images were taken at intervals of 0.7 s immediately after bleaching, increasing to 4.0 s at the end of a run, when the fluorescence distribution varied slowly.

A 40 × 1.3 numeric aperture objective (Nikon Inc., Melville, NY) was used, and all images were taken focused at the "equator" or midplane of the spherical cells. Because of the large numeric aperture of this lens, the image of the bleached pattern is formed only from that part of the cell within the depth of field, ±2 μm. This distance was determined by bleaching a thin fluorescent sample (Schneider and Webb, 1981) and then defocusing until this bleached pattern was no longer visible. The imaging device used was a CCD camera (CC200, Photometrics Ltd., Tucson, AZ; CSF TH7882CDA chip, Thomson Instrument Co., Newark, DE), output digitized to 12 bits. Only a small 128-pixel × 128-pixel region of the chip was used for images, which corresponded to a 50-μm × 50-μm area of the microscope field. This format allows a more rapid readout of the camera. Digital images were transferred to an image processor.

Analysis of fluorescence images

To determine whether protein diffusion depends on concentration, both local protein concentrations and diffusion coefficients were determined from fluorescence images. Local protein concentrations were estimated from a prebleach image (Fig. 2 a). Protein distributions on electrophoresed cells have been discussed by Ryan et al. (1988). They showed that the protein concentration on a spherical cell in the presence of an electric field is best fit by a Fermi-Dirac or excluded-volume distribution:

$$\frac{C(\theta)}{C_0} = \frac{(1-x_e)/f_0}{e^{-\mu/k_B T}e^{\beta\cos\theta/k_B T} + 1} + x_e, \qquad (1)$$

where $C(\theta)$ is the protein concentration at an angle θ from the anodal pole of the cell, C_0 is the mean protein concentration, x_e is the fraction of protein that is electrophoretically immobile, f_0 is the fractional area covered by protein (averaged over the cell surface), β is the coupling to the electric field, and μ is a chemical potential. This distribution has a characteristic "flat top," which reflects crowding of protein at the cathodal pole. The mean protein concentration, C_0, was determined by
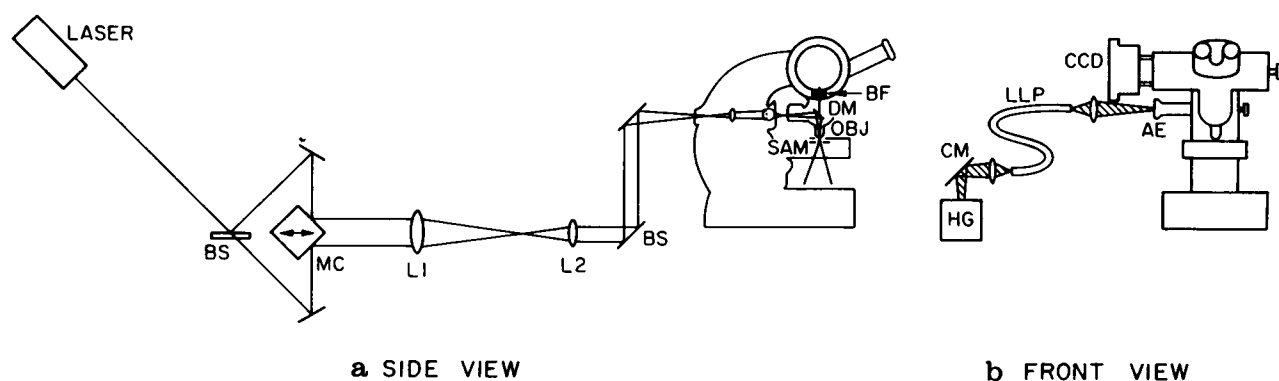

a SIDE VIEW   b FRONT VIEW

FIGURE 1   Bleaching apparatus. The 514-nm line from a Coherent Innova-6 argon ion laser is split by the beamsplitter (BS). The spacing of parallel beams is controlled by moving a mirrored cube (MC); those beams are crossed in an auxilliary field plane by lenses L1 and L2. A beam steering device (BS) sends the beams through the primary epiport of a Zeiss Universal microscope. A dichroic mirror (DC) and barrier filter (BF) are used as in conventional epifluorescence microscopy. SAM, sample, OBJ, 40× 1.3 numeric aperture. For postbleach images, illumination is provided by a mercury lamp (HG), with a cold mirror (CM) and a liquid light pipe scrambler (LLP). Light enters via a Zeiss auxilliary epiport (AE). Images are taken with the Photometrics CC200 CCD (CCD).

an integration over the cell surface; that is,

$$C_0 = \frac{1}{4\pi r^2} \int\int C(\theta)dS, \qquad (2)$$

where it has been assumed that the cell is spherical with radius r and the protein distribution is a function of θ only. In the work by Ryan et al., fluorescence profiles around the cell were first normalized to this mean fluorescence intensity and then fit to Eq. 1.
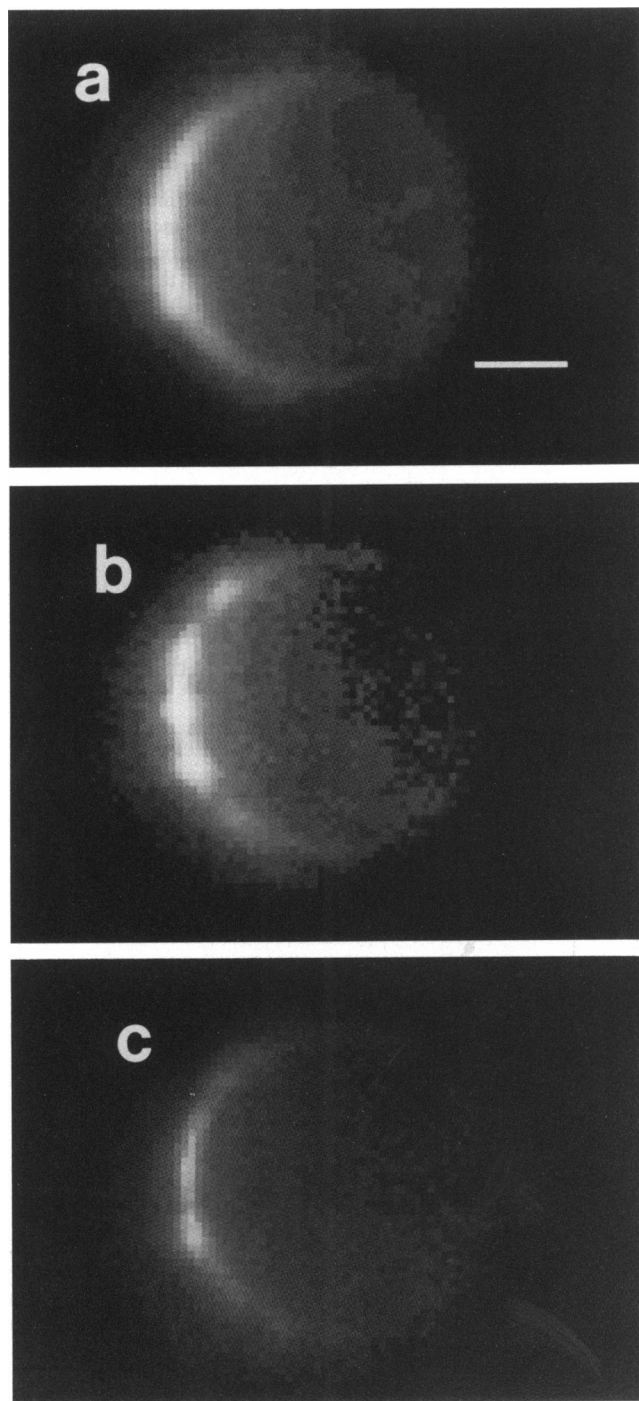
We have utilized this approach to characterize the apparent area covered with protein in the TRITC-IgE$_R$–labeled RBL cell and to compare the degree of electrophoresis (β) of Con A receptors with that of liganded IgE$_R$ receptors. However, since Eq. 1 has four fitting parameters (x_e, f_0, β, and μ), the determination of the precise degree of crowding on a single cell is not robust: a small uncertainty in the profile may yield large changes in parameter values. To avoid this problem, we have chosen to characterize protein concentrations on individual cells in a model-independent way, expressing them as ratios to the mean cell surface protein concentration. This mean concentration is calculated as the integral of the fluorescence over the cell surface (assumed spherical), as in Eq. 2. Experimentally, RBL cells remain nearly spherical for up to 1 h at room temperature after plating onto glass coverslips. (This was determined by measuring the ventral-to-dorsal cell diameter with a calibrated focus control. This diameter decreased < 20% over the course of 1 h at room temperature.)

Diffusion coefficients were determined by measuring the decay, in time, of the periodic pattern bleached into the cell (Fig. 2, b and c). Because the region of intersection of the laser beams has an extent of several hundred microns along the optic axis, areas of the cell above and below the plane of focus are bleached with the same pattern as the in-focus region. Consequently, diffusional recovery at the poles of the cell is due to a redistribution in the plane of focus and not a flux from or to other focal planes. We are therefore justified in treating this as a one-dimensional diffusion problem, with θ as the only spatial variable. (Analysis of diffusion kinetics on other regions of the cell, e.g., the sides, would require a complete solution of the diffusion equation in terms of its eigenfunctions on a sphere, the spherical harmonics. By restricting our attention to the poles of the cell, we reduce the dimensionality.)

The fringe pattern bleaches a periodic fluorescence profile into the cell. The peak-to-peak spacing, along the equator, varies with position around the cell, as seen in Figs. 2 b and 3 a. The bleached pattern, as a function of θ, therefore contains a distribution of spatial frequencies. However, each spatial frequency is decoupled from the others in the one-dimensional diffusion equation, so that each, by itself, could in principle provide a measure of D. Near the poles of each cell, the pattern spacing is nearly constant; the Fourier transform exhibits a peak at this spatial frequency (Fig. 3 c). The diffusion coefficient and immobile fraction are determined from the decay of this peak. The decay is well fit to the solution of the diffusion equation in Fourier space:

$$F(k, t) = F(k, 0)[(1 - x_p)e^{-Dk^2 t} + x_p], \qquad (3)$$

where $F(k, t)$ is the amplitude of spatial frequency k, t is time, x_p is a fraction of protein that is immobile by fluorescence photobleaching recovery, and D is the diffusion coefficient. The amplitudes $F(k, t)$ are determined from the cell images by a fast Fourier transform of

FIGURE 2   Equatorial fluorescence distributions. (a) Prephotobleach image of the equilibrium distribution of TRITC-labeled IgE-R on an RBL cell in an applied electric field of strength 3.75 V/cm. The image was taken by focusing at the midplane of the spherical cell. The polar angle θ is measured from the dim pole. For an exactly spherical cell, the fluorescence will be a function of θ only, so that the entire surface distribution can be characterized by measuring the fluorescence at the mid-plane for each θ. (b) First postbleach image of the cell in a. The pattern has been bleached into the entire cell, both above and below the plane of focus seen here. Consequently, diffusional recovery at the poles occurs by redistribution in θ only, and the problem reduces to one dimension. (c) The same cell, 42 s after photobleaching. Bar, 5 μm.
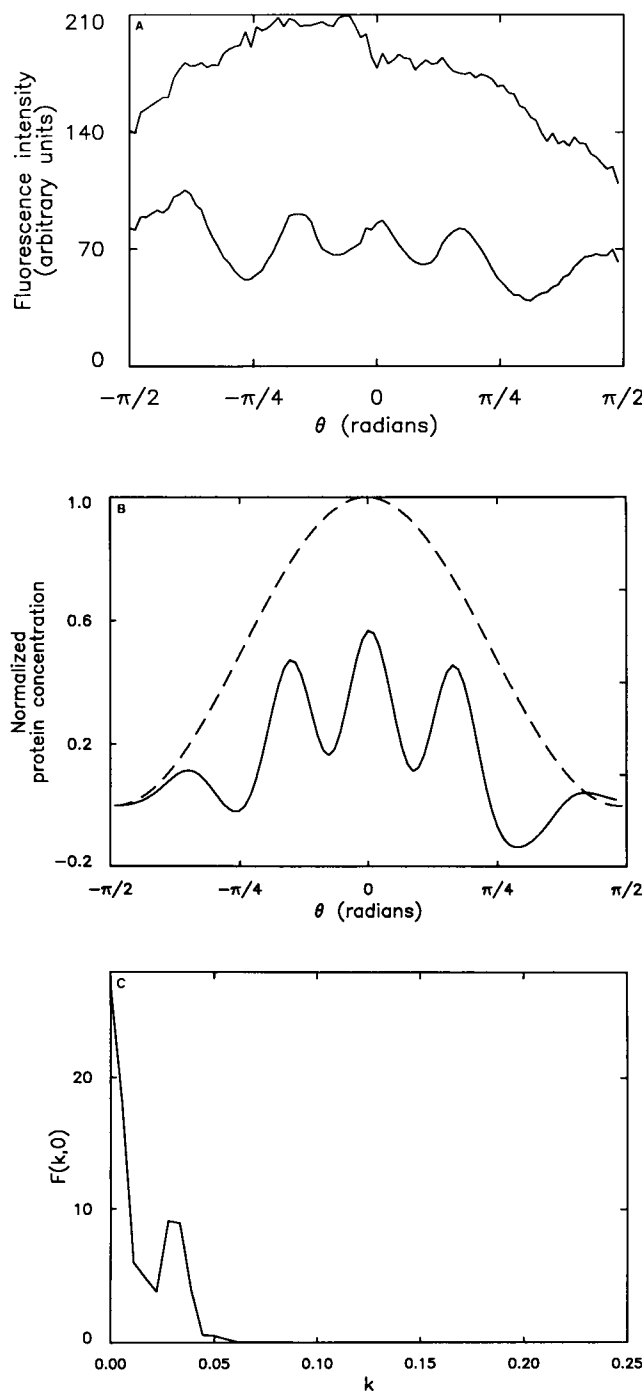
fluorescence profiles, $C(\theta, t)$:

$$F(k, t) = \left| \int_{-\pi/2}^{\pi/2} H(\theta) \cdot C(\theta, t) e^{-ik\theta} \, d\theta \right| . \qquad (4)$$

The integral covers either the cathodal or the anodal half of the cell, and the function $H(\theta)$ is a "Hanning Window" ($\sim \cos \theta$) included to improve spectral quality (Press et al., 1986) (Fig. 3 b). The peak in the Fourier transform amplitudes due to the bleached pattern is evident in Fig. 3 c. The $F(k, t)$ are determined by measuring the magnitude of this peak at each postbleach time point. The $F(k, t)$ values for the cathodal half of one cell are graphed in Fig. 4. These values are fit to Eq. 3 to obtain the three parameters $F(k, 0)$, Dk^2, and x_p. The value of k is known from measurements of the bleach pattern periodicity, L:

$$k = \frac{2\pi}{L} . \qquad (5)$$

D is then easily computed.

For both protein concentration measurements and diffusion measurements, circumferential intensity profiles were obtained by measuring the mean fluorescence in a wedge-shaped window from θ to $\theta + 2°$ and $r - \delta r$ to r, for each position θ around the cell. Using the mean intensity from a block of pixels, rather than a single pixel value, eliminates errors due to bloom distortion and reduces shot noise in the $F(\theta)$ profiles. The window size δr is chosen to encompass the full width of the fluorescent equatorial ring and is positioned automatically to sample the maximum intensity, which occurs at the periphery of the cell.

RESULTS

To demonstrate that the redistribution of IgE receptor toward the cathode in an electric field is typical of RBL membrane proteins, we labeled cells with Rh-S-Con A
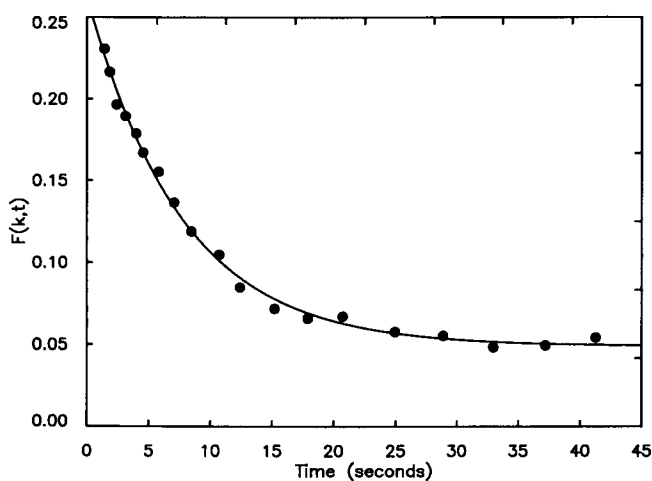

FIGURE 3 Intensity profiles and transform from an intact cell. (*A*) Circumferential intensity profiles of the cathodal half of an intact electrophoresed RBL cell, before (*upper curve*) and immediately after photobleaching (*lower curve*). (*B*) Windowed fluorescence circumferential intensity of the postbleach curve from *a*, after high spatial frequency noise has been filtered out. The dashed line is the Hanning window. (*C*) The magnitude of the Fourier transform of the profile in *b*. The *x*-axis is in cycles per degree. The peak at 0.03 corresponds to 1 cycle per 30°, the dominant bleached spatial frequency in *b*.

FIGURE 4 Time course of the decay of the bleaching Fourier component in Fig. 3 c. The area under the peak decays with time (●) and is well fit with a single exponential (*solid curve;* $\tau = 20$ s) and an immobile component (15%).

after a 20-min exposure to a 20 V/cm field. All cells showed a dramatic cathodal redistribution of Con A receptors. The mean fluorescence enhancement at the cathodal pole was a factor of 2.7, only slightly smaller than the 3.4 obtained with prefield-labeled IgE_R-receptor complex at this field strength. These results, and those of Ryan et al. (1988), indicate that accumulation of IgE_R-R in our experiments reflects a general increase in overall protein concentration and not a specific accumulation of one labeled constituent.

Measurements of diffusion coefficients and immobile fractions for normal RBL cells are presented in Fig. 5. The extent of crowding is characterized by the normalized fluorescence intensity, C/C_0, where C is the fluorescence intensity at the pole, and C_0 is the mean cell surface fluorescence intensity, computed from the integral in Eq. 2. The rhodamine fluorophore does not self quench at these concentrations, so that the fluorescence intensity is proportional to the IgE-R surface concentration. A variety of field strengths, from 4 to 20 V/cm, were used to obtain the range of concentrations reported. The scatter in the measurements of D is consistent with previous work on this system (Menon et al., 1986). We obtain $D = (4.6 \pm 2.5) \times 10^{-10}$ cm^2/s, and we find no significant correlation of D with protein concentration.

For many of the cells represented in Fig. 5, diffusion

measurements were feasible only on the bright, cathodal pole of the cell; the anodal pole becomes too depleted to make a meaningful estimate of tracer diffusion there. To determine whether the broad range of cell-to-cell variability in D obscures a subtle concentration dependence, we have plotted the ratios of diffusion coefficients at opposite poles of individual cells in Fig. 6 a, for those cells on which an accurate determination of the diffusion coefficient at the sparse anodal pole was possible. The abscissa is the normalized fluorescence intensity at the bright, cathodal pole of the cell. This figure again shows that there is no significant correlation of the diffusion rate of TRITC-IgE-R with local protein concentration in single RBL cells.

Ratios of immobile fractions for the cells included in Fig. 6 a are presented in Fig. 6 b. The average ratio of cathodal to anodal immobile fractions is 0.88. A reduc-
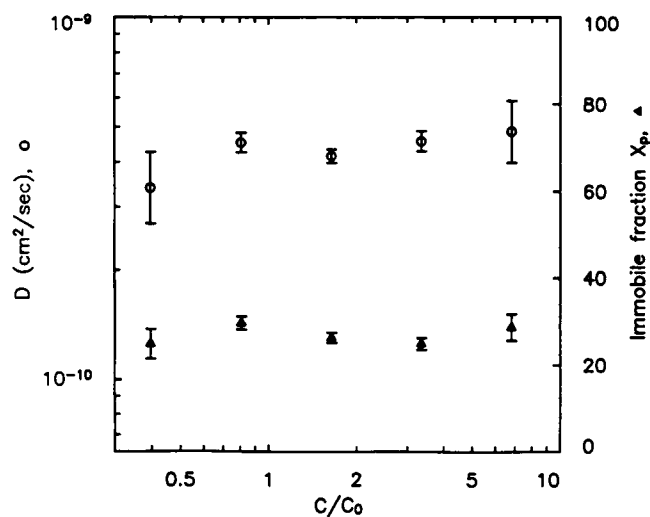

FIGURE 5 Diffusion coefficients (O) and immobile fractions (▲) for all intact cells measured. The data have been binned into five divisions. Each symbol is an average value for many observations (total of 209 measurements); the uncertainties indicated are SEMs. The degree of crowding is measured by the normalized fluorescence intensity, F/F_0. The dim anodal poles of cells have $F/F_0 < 1$, whereas the bright cathodal ends have $F/F_0 > 1$.
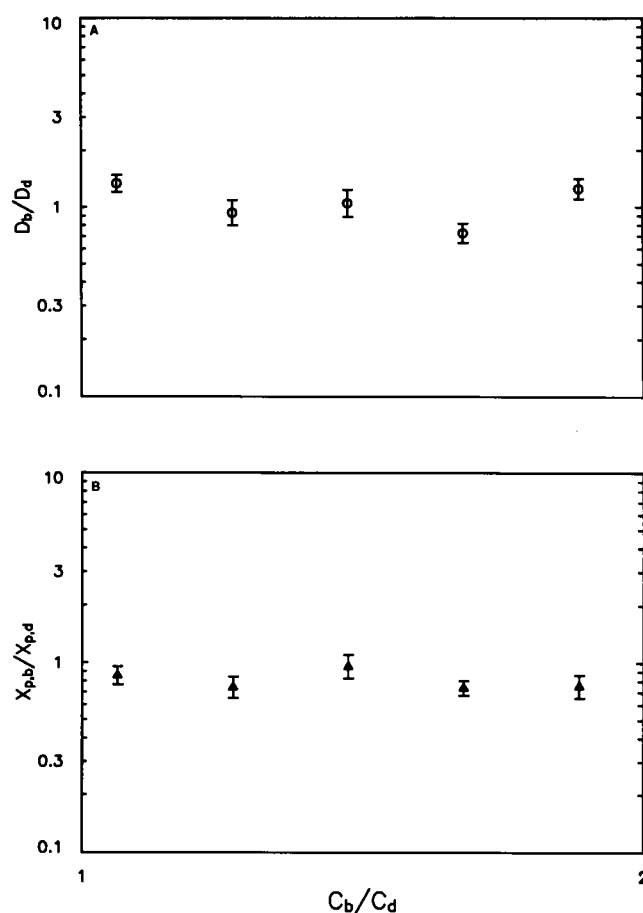

FIGURE 6 Ratios of diffusion data on intact cells. (a) Ratios of diffusion coefficients for cells in which an accurate determination was possible for both the bright and dim poles. Means and SEMs of the data binned into five concentration ranges are shown. (b) Ratios of immobile fractions for cells presented in a. Data from 60 cells.
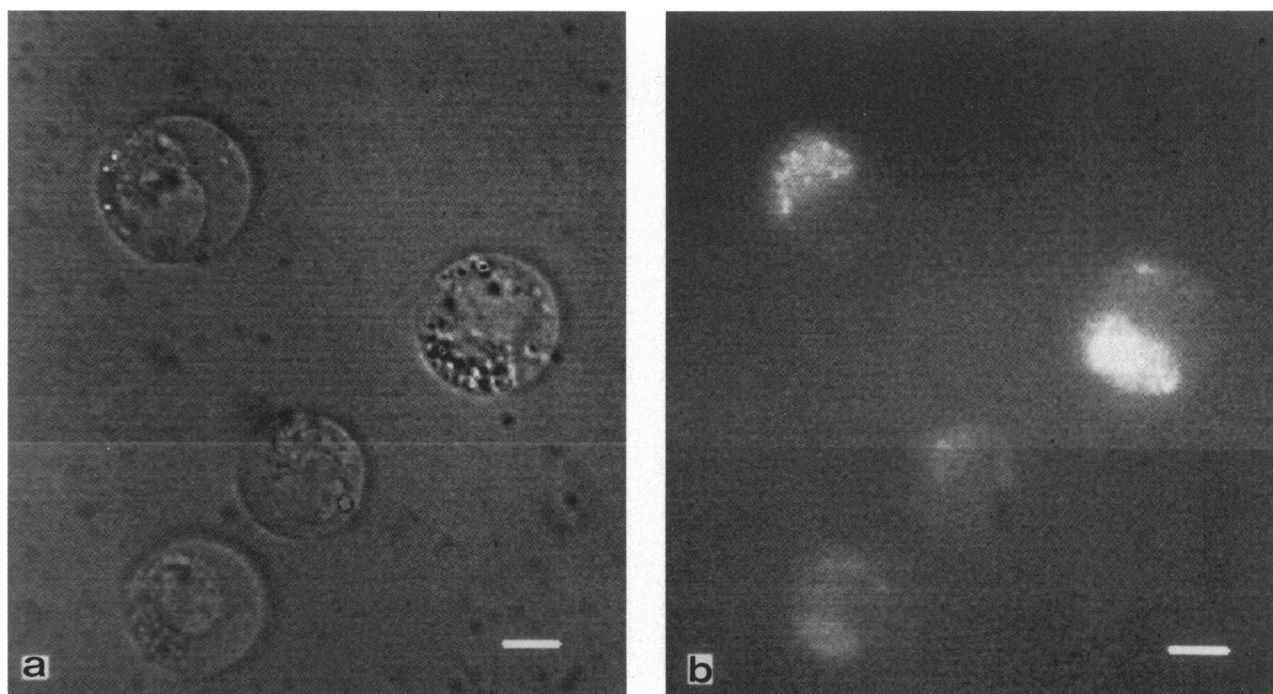
FIGURE 7   Micrographs of osmotically swollen cells in (a) bright field, showing separation of plasma membrane from cytosolic constituents, and (b) with the actin cytoskeleton fluorescently labeled with Bodipy-phallacidin. Bar, 10 μm.

tion in immobile fraction is expected for the bright cathodal end of the cell, because electrophoretically mobile protein is added to that region. Conversely, the immobile fraction increases at the dim anodal pole since mobile proteins are being depleted from that region. The immobile proteins are uniformly distributed, and hence the number densities at the two poles remain equal. Except for a few wildly varying values, we find this to be true.

To investigate the possibility that cytoskeletal involvement in protein diffusion suppresses or overwhelms concentration dependence effects, we have made the same measurements on hypoosmotically shocked cells. We verified that the cell membranes do in fact separate from the subplasmalemmal actin cytoskeleton by fluorescence labeling F-actin with Bodipy phallacidin; see Fig. 7. The mean value for D on bulbous cells that have not been exposed to an electric field is 2×10^{-9} cm^2/s, about five times faster than on intact cells. Diffusion coefficients and immobile fractions measured on these bulbous cells are presented in Fig. 8. A decrease in self diffusion with crowding is evident. The reduction in the immobile fraction with increased concentration again reflects the addition of electrophoretically mobile protein to the crowded pole of the cell. The ratios of diffusion coefficients are presented in Fig. 9 a. There is a
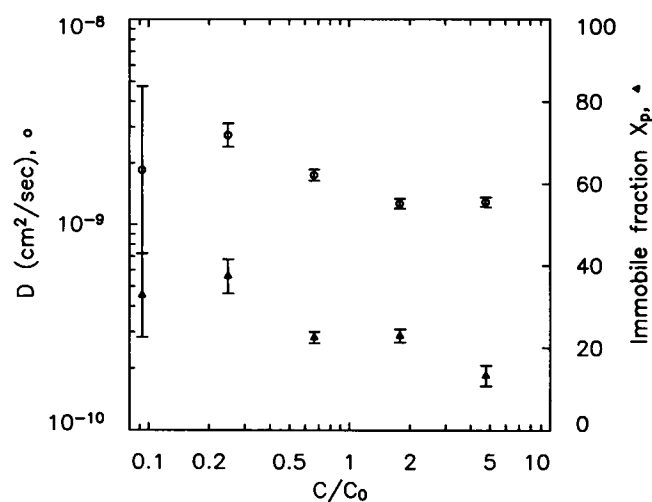

FIGURE 8   Diffusion coefficients (O) and immobile fractions (▲) for all measurements on swollen cells. The data have been binned into five divisions. Each symbol is an average value for many observations (total of 269 measurements); the uncertainties indicated are SEMs. The degree of crowding is measured by the normalized fluorescence intensity, F/F_0. The dim anodal poles of cells have $F/F_0 < 1$, whereas the bright cathodal ends have $F/F_0 > 1$.
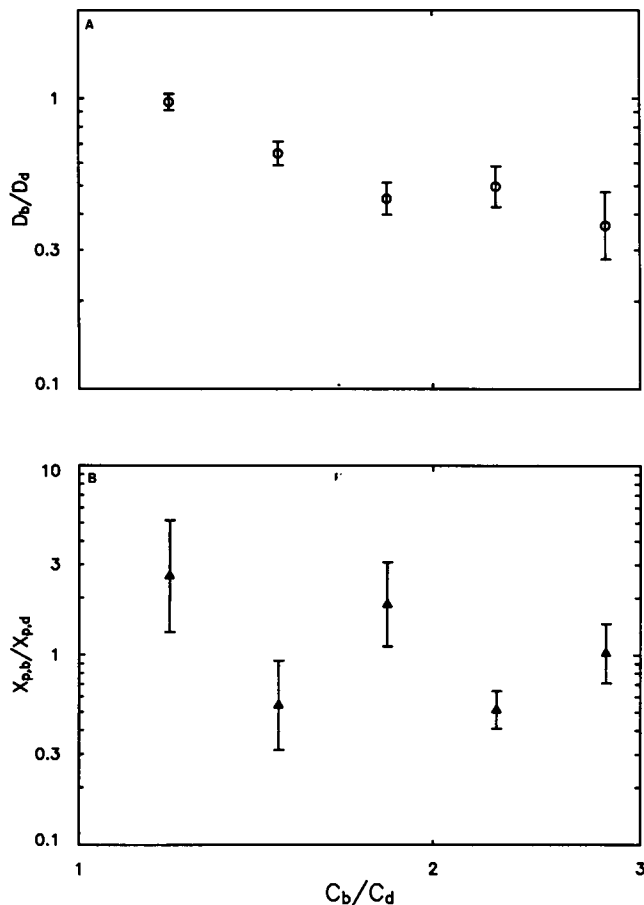
FIGURE 9 Ratios of diffusion data on swollen cells. (a) Ratios of diffusion coefficients for 87 bulbous cells. Means and SEMs of the data binned into five concentration ranges are shown. (b) Ratios of immobile fractions for the same 87 cells.

significant dependence on concentration, with the most crowded regions showing up to a fourfold reduction in lateral diffusibility. Ratios of the immobile fractions corresponding to the data in Fig. 9 a are plotted in Fig. 9 b.

DISCUSSION

Our data show that a concentration dependence of the diffusion coefficient of IgE_R-R can be observed on bulbous cells, where reduction of cytoskeletal interactions speeds diffusion by a factor of five. Here, when the protein concentration is increased threefold by electrophoretic segregation, the IgE_R-R diffusion slows by a factor of four. On intact cells, however, no dependence of D on protein concentration was found within experimental uncertainty.

The observations on osmotically swollen cells are in general agreement with a number of Monte Carlo computer experiments (Pink, 1985; Saxton, 1987, 1989; Donaldson, 1989), as well as with experiments on reconstituted membrane protein systems (Peters and Cherry, 1982; Tank et al., 1982a). To compare our observations with these studies, we used the method of Ryan et al. (1988) to determine the fraction of accessible cell surface area that is occupied by electrophoresable protein. The TRITC-IgE_R fluorescence profiles on electrophoresed (unbleached) cells were fit to a Fermi-Dirac excluded volume distribution (Eq. 1). The mean protein area fraction was found to be ~ 10–20% on both intact and bulbous cells. (This is in accord with biochemical estimates of protein concentrations [Golan et al., 1984; Quinn et al., 1984].) Cathodal ends of electrophoresed cells have protein area fractions exceeding 30–60%. Saxton (1989) has reported that these concentrations should reduce tracer diffusion by a factor of two to five; other Monte Carlo experiments have yielded similar results. In reconstituted systems, the diffusion coefficients of gramicidin C (Tank et al., 1982a) and bacteriorhodopsin (Peters and Cherry, 1982) in dimyristoyl phosphatidylcholine bilayers are both attenuated by about a factor of three when protein area fractions are increased above $\sim 20\%$.

What differences are there between osmotically swollen and intact RBL cells that could account for the absence of detectable concentration dependence of the protein diffusion coefficient in intact cells? We have demonstrated through fluorescence microscopy that the cell membrane is pulled away from the subplasmalemmal actin cytoskeleton by the osmotic shock. The actin cytoskeleton may slow IgE_R-R diffusion in intact cells, but may be ineffectual in the osmotically swollen cells. Thus, the removal of this source of restraint exposes the concentration dependence of diffusion coefficients on the concentration of membrane protein. Monte Carlo computer models as well as theoretical considerations suggest that this is reasonable. For example, Saxton (1989) has found that a given concentration of immobile obstacles reduces D much more than the same concentration of mobile ones. When there are weak attractive interactions, immobile obstacles should dominate diffusion. This is because the transient binding of a protein to an immobile obstacle will arrest diffusion entirely, during the lifetime of the bond, whereas the transient binding of two mobile proteins to each other should reduce their diffusion coefficient by only a few percent, according to the logarithmic size dependence of D derived by Saffman and Delbrück (1975). (A formal treatment of the effects of chemical binding on diffusion has been presented by Elson and Magde [1974]; the text by Crank [1975] discusses the fast reaction limit.)

A number of experiments on cells have demonstrated that removal of cytoskeletal constraints can result in greatly enhanced diffusion of proteins. Tank et al. (1982b) removed constraints by creating blebs, or bubble-like protrusions, of cell membrane. The blebs were created on L6 myoblast membranes by treatment with 25 mM formaldehyde, 2 mM DTT in PBS. On these blebs, Con A receptors and acetylcholine receptors diffuse rapidly (0.4 and 0.3 $\mu m^2/s$, respectively); on intact cells these proteins diffuse at 0.004 and 0.05 $\mu m^2/s$ (Schlessinger et al., 1976). These blebs have a protein and lipid composition similar to that of intact cell membrane; these dramatic increases in diffusion cannot be explained by a protein concentration effect. Barak and Webb (1982) chemically treated human fibroblasts to induce blebs. In untreated cells, they found that the LDL receptor diffused at ~ 0.004 $\mu m^2/s$; on blebbed regions of treated cells, diffusion of this receptor speeded up to 0.2 $\mu m^2/s$. Wu et al. (1982) were able to remove cytoskeletal constraints on lymphocytes and RDM_4 lymphomas by incubation with Con A. A subpopulation of 10 to 20% of the cells was found to develop blebs, which swelled to envelop the entire cell within 2–3 h. Labeling with NBD-phallacidin (7-nitrobenz-2-oxa-1,3-diazole-phallacidin) indicated that the membrane had expanded well above the subplasmalemmal actin cytoskeleton. In these cells, Con A receptors were found to diffuse at 0.9 $\mu m^2/s$ with essentially complete mobility. On cells that had not swollen, Con A receptors were immobile.

Concentration-dependent diffusion in reconstituted, cytoskeleton-free systems has been well established, as has the ability of the cytoskeleton to attenuate cell surface protein diffusion coefficients by two to three orders of magnitude. Our novel result is that protein concentration differences have a negligible effect on diffusion when cytoskeletal structures remain intact. The intact cytoskeleton, or some surrogate membrane feature, such as the membrane matrix described by Mescher et al. (1981) and Apgar and Mescher (1986), apparently dominates diffusive behavior in the RBL cell. In addition, the cytoskeleton can immobilize a significant fraction of the cell surface protein, preventing its redistribution in the electric field. As much as 77% of RBL cell surface protein may be electrophoretically immobile, as determined by Ryan et al. (1988) with a nonspecific polyclonal anti-RBL antibody. Our estimates of the protein concentrations at opposite poles of the cell are based on the concentration gradients of the IgE receptor, which is almost completely electromobile. Consequently, total protein concentrations may vary only one-fifth as much as the concentration of IgE receptor. This fact, and computer experiments that show that the immobile protein concentration affects D more than the mobile protein concentration, may contribute

to the absence of detectable diffusion modulation in intact RBL cells.

It is illuminating to compare our results with work by Yechiel and Edidin (1987) on living human skin fibroblasts. They noted a dramatic, sixfold decrease in protein diffusion in regions of high protein concentration. These regions, which they suggest are ~ 1 μm in size, preexist in the plasma membrane, as indicated by variation in the intensity of labeling by a nonspecific anti-human antibody. The regions of higher protein concentration cannot be explained by patches of immobile protein, since immobile fractions in both low and high concentration regions are about the same ($\sim 50\%$). Yechiel and Edidin postulate the existence of immiscible, presumably fluid, domains and suggest that proteins are unable to diffuse freely between protein-rich and protein-poor domains.

These results on human skin fibroblasts suggest a concentration-dependent diffusivity in intact cells with intact cytoskeletal architecture (as evidenced by the large immobile populations). This is in apparent contrast to our lack of such dependence in the intact RBL system. However, two distinguishing features require consideration. First, even though the immobile fractions in both the high- and low-density domains are the same, the number density of immobile proteins must be higher in the high-density domain. Consequently, the rate of interaction of a mobile constituent with an immobile obstacle will be higher in the concentrated regions than in the dilute regions. It is not possible to determine from the data to what extent the interaction with these immobile constituents is responsible for the observed reduction in D. Furthermore, the protein-rich domains on these fibroblasts must be homeostatic; the cells maintain these regions against entropic forces by mechanisms that are not yet understood. In contrast, electroosmotically induced protein concentration gradients are not stabilized, and relaxation through back diffusion begins immediately on removal of the field. The factors that play a role in the maintenance of a protein-rich domain in a fibroblast might also affect protein diffusion from that domain.

The experiments of Yechiel and Edidin on fibroblasts are complementary to our experiments on RBL cells. We have created regions of high mobile protein concentration; the fibroblast cell experiments probe regions of high total protein concentration, mobile and immobile. The concentration gradient of mobile protein on the RBL cell is maintained by the external field, whereas the concentration variations probed in the fibroblast are native structures of the cell.

Last, it is important to acknowledge that other variables, besides protein concentration, may have a significant effect on diffusion in bulbous cells. In particular, a

membrane matrix has been found in this (Apgar, 1990) and other (Apgar and Mescher, 1986) cell lines. It may dominate protein diffusion in cell surfaces. Antigen-crosslinked IgE receptors associate with this membrane skeleton in RBL cells and become insoluble by TX-100 detergent. Uncrosslinked receptors, such as those examined in this study, retain detergent solubility; nonetheless, monomeric receptors may still retain some degree of interaction with the membrane skeleton. If the membrane skeleton is only partially disrupted by osmotic shock, subsequent exposure to the electric field might result in cathodal migration of the skeletal fragments due to their interaction with membrane proteins that protrude into the electroosmotic flow. If this occurs, a reduction in diffusion coefficient at the cathodal end would be expected due to interactions of membrane proteins with these fragments. In intact cells, the structure would not be free to realign and consequently could not differentially affect diffusion at the cathodal and anodal ends.

Conclusions

We report an apparent dependence of D on protein concentration for the IgE receptor complex on bulbous RBL cells, formed by hypoosmotic shock, but we find no apparent dependence on intact cells (within the uncertainties of the measurement and the variation of the biological system). Hypoosmotically shocked cells suffer a disruption of normal cytoskeletal architecture, as shown by fluorescence microscopy and by the enhancement of IgE receptor diffusion. The concentration dependence of D in the disrupted cells is in accord with previous measurements on reconstituted membrane protein systems and with Monte Carlo computer experiments. The absence of such a concentration dependence on intact cells suggests that cytoskeletal or membrane matrix factors may play a dominant role in establishing the mobility of this receptor on the intact cell, presumably through indirect or very weak interactions.

REFERENCES

Apgar, J. R. 1990. Antigen-induced cross-linking of the IgE receptor leads to an association with the detergent-insoluble membrane skeleton of rat basophilic leukemia (RBL-2H3) cells. *J. Immunol.* 145:3814–3822.

Apgar, J. R., and M. F. Mescher. 1986. Agorins: major structural proteins of the plasma membrane skeleton of P815 tumor cells. *J. Cell Biol.* 103:351–360.

Barak, L. S., and W. W. Webb. 1982. Diffusion of low density lipoprotein-receptor complex on human fibroblasts. *J. Cell Biol.* 95:846–852.

Crank, J. 1975. *In* The Mathematics of Diffusion. Clarendon Press, Oxford. 326–351.

Davoust, J., P. F. Devaux, and L. Leger. 1982. Fringe pattern photobleaching: a new method for the measurement of transport coefficients of biological macromolecules. *EMBO (Eur. J. Mol. Biol. Organ.)* 1:1233–1238.

Donaldson, P. 1989. Ph.D. thesis. Cornell University, Ithaca, New York.

Elson, E. L., and D. Magde. 1974. Fluorescence correlation spectroscopy I. *Biopolymers.* 13:1–27.

Golan, D. E., M. R. Alecio, W. R. Veatch, and R. R. Rando. 1984. Lateral mobility of phospholipid and cholesterol in the human erythrocyte membrane: effects of protein-lipid interactions. *Biochemistry.* 23:332–339.

Jaffe, L. F. 1977. Electrophoresis along cell membranes. *Nature (Lond.).* 265:600–602.

McCloskey, M. A., Z.-Y. Liu, and M-m. Poo. 1984. Lateral electromigration and diffusion of Fcε receptors on rat basophilic leukemia cells: effects of IgE binding. *J. Cell Biol.* 99:778–787.

McLaughlin, S., and M-m. Poo. 1981. The role of electro-osmosis in the electric-field–induced movement of charged macromolecules on the surfaces of cells. *Biophys. J.* 31:85–93.

Menon, A. K., D. Holowka, W. W. Webb, and B. Baird. 1985. Clustering, mobility and triggering activity of small oligomers of IgE on rat basophilic leukemia cells. *J. Cell Biol.* 102:534–540.

Menon, A. K., D. Holowka, W. W. Webb, and B. Baird. 1986. Cross-linking of receptor-bound IgE to aggregates larger than dimers leads to rapid immobilization. *J. Cell Biol.* 102:541–550.

Mescher, M. F., M. J. L. Jose, and S. P. Balk. 1981. Actin-containing matrix associated with the plasma membrane of murine tumour and lymphoid cells. *Nature (Lond.).* 289:139–144.

Okada, C. Y., and M. Rechsteiner. 1982. Introduction of macromolecules into cultured mammalian cells by osmotic lysis of pinocytic vesicles. *Cell.* 29:33–41.

Peters, R., and R. J. Cherry. 1982. Lateral and rotational diffusion of bacteriorhodopsin in lipid bilayers: experimental test of the Saffman-Delbrück equations. *Proc. Natl. Acad. Sci. USA.* 79:4317–4321.

Pfeiffer, J. R., J. C. Seagrave, B. H. Davis, G. G. Deanin, and J. M. Oliver. 1985. Membrane and cytoskeletal changes associated with IgE-mediated serotonin release from rat basophilic leukemia cells. *J. Cell Biol.* 101:2145–2155.

Pink, D. A. 1985. Protein lateral movement in lipid bilayers. Simulation studies of its dependence upon protein concentration. *Biochim. Biophys. Acta.* 818:200–204.

Poo, M-m., J. W. Lam, N. Orida, and A. W. Chao. 1979. Electrophoresis and diffusion in the plane of the cell membrane. *Biophys. J.* 26:1–21.

Press, W. H., B. P. Flannery, S. A. Teukolsky, and W. T. Vetterling. 1986. *In* Numerical Recipes. Cambridge University Press, Cambridge. 420–429.

Quinn, P., G. Griffiths, and G. Warren. 1984. Density of newly synthesized plasma membrane proteins in intracellular membranes. II. Biochemical studies. *J. Cell Biol.* 98:2142–2147.

Ryan, T. A., J. Myers, D. Holowka, B. Baird, and W. W. Webb. 1988. Molecular crowding on the cell surface. *Science (Wash. DC)*. 239:61–64.

Saffman, P. G., and M. Delbrück. 1975. Brownian motion in biological membranes. *Proc. Natl. Acad. Sci. USA*. 72:33111–3113.

Saxton, M. J. 1987. Lateral diffusion in an archipelago: the effect of mobile obstacles. *Biophys. J.* 52:989–997.

Saxton, M. J. 1989. Lateral diffusion in an archipelago: distance dependence of the diffusion coefficient. *Biophys. J.* 56:615–622.

Schlessinger, J., D. E. Koppel, D. Axelrod, K. Jacobson, W. W. Webb, and E. L. Elson. 1976. The lateral mobility of concanavalin A receptors on myoblasts. *Proc. Natl. Acad. Sci. USA*. 73:2409–2413.

Schneider, M. B., and W. W. Webb. 1981. Measurement of submicron laser beam radii. *Applied Optics*. 20:1382–1388.

Tank, D. W., E. S. Wu, P. Meers, and W. W. Webb. 1982a. Lateral diffusion of gramicidin C in phospholipid multibilayers. *Biophys. J.* 40:129–135.

Tank, D. W., E. S. Wu, and W. W. Webb. 1982b. Enhanced molecular diffusibility in muscle membrane blebs: release of lateral constraints. *J. Cell Biol.* 92:207–212.

Webb, W., L. S. Barak, D. W. Tank, and E.-S. Wu. 1981. Molecular mobility on the cell surface. *Biochem. Soc. Symp.* 46:191–205.

Wu, E.-S., D. W. Tank, and W. W. Webb. 1982. Unconstrained lateral diffusion of concanavalin A receptors on bulbous lymphocytes. *Proc. Natl. Acad. Sci. USA*. 79:4962–4966.

Yechiel, E., and M. Edidin. 1987. Micrometer-scale domains in fibroblast plasma membranes. *J. Cell Biol.* 105:755–760.

Zhang, F., B. Crise, D. A. Brown, Y. Hou, J. Rose, and K. A. Jacobson. 1990. Lateral mobility of lipid linked and transmembrane proteins in transfected COS-1 cells. *Biophys. J.* 57:287a. (Abstr.)